



Contents lists available at ScienceDirect

## Biochemical and Biophysical Research Communications

journal homepage: [www.elsevier.com/locate/ybbrc](http://www.elsevier.com/locate/ybbrc)Isopentenyl pyrophosphate secreted from Zoledronate-stimulated myeloma cells, activates the chemotaxis of  $\gamma\delta$ T cellsEishi Ashihara<sup>a,b,\*</sup>, Tatsuya Munaka<sup>c,1</sup>, Shinya Kimura<sup>d</sup>, Saori Nakagawa<sup>e</sup>, Yoko Nakagawa<sup>b</sup>, Masaki Kanai<sup>c</sup>, Hideyo Hirai<sup>b</sup>, Hirohisa Abe<sup>c</sup>, Takashi Miida<sup>f</sup>, Susumu Yamato<sup>e</sup>, Shuichi Shoji<sup>g</sup>, Taira Maekawa<sup>b</sup><sup>a</sup> Department of Clinical and Translational Physiology, Kyoto Pharmaceutical University, Kyoto, Japan<sup>b</sup> Department of Transfusion Medicine and Cell Therapy, Kyoto University Hospital, Kyoto, Japan<sup>c</sup> Technology Research Laboratory, Shimadzu Corporation, Kyoto, Japan<sup>d</sup> Division of Hematology, Respiratory Medicine and Oncology, Department of Internal Medicine, Faculty of Medicine, Saga University, Saga, Japan<sup>e</sup> Department of Bio-analytical Chemistry, Faculty of Pharmaceutical Sciences, Niigata University of Pharmacy and Applied Life Sciences, Niigata, Japan<sup>f</sup> Department of Clinical Laboratory Medicine, Juntendo University School of Medicine, Tokyo, Japan<sup>g</sup> Department of Electronic and Photonic Systems, Waseda University, Tokyo, Japan

## ARTICLE INFO

## Article history:

Received 11 May 2015

Accepted 30 May 2015

Available online 3 June 2015

## Keywords:

 $\gamma\delta$ T cells

Chemotaxis

Tumor immunity

Multiple myeloma

Isopentenyl pyrophosphate

## ABSTRACT

$\gamma\delta$ T cell receptor (TCR)-positive T cells, which control the innate immune system, display anti-tumor immunity as well as other non-immune-mediated anti-cancer effects.  $\gamma\delta$ T cells expanded *ex vivo* by nitrogen-containing bisphosphonate (N-BP) treatment can kill tumor cells. N-BP inhibits farnesyl pyrophosphate synthase in the mevalonate pathway, resulting in the accumulation of isopentenyl pyrophosphate (IPP), which is a stimulatory antigen for  $\gamma\delta$ T cells. We have previously observed that as they get closer, migrating  $\gamma\delta$ T cells increase in speed toward target multiple myeloma (MM) cells. In the present study, we investigated the  $\gamma\delta$ T cell chemotactic factors involving using a micro total analysis system-based microfluidic cellular analysis device. The addition of supernatant from RPMI8226 MM cells treated with the N-BP zoledronic acid (ZOL) or the addition of IPP to the device induced chemotaxis of  $\gamma\delta$ T cells and increased the speed of migration compared to controls. Analysis of the ZOL-treated RPMI8226 cell supernatant revealed that it contained IPP secreted in a ZOL-dose-dependent manner. These observations indicate that IPP activates the chemotaxis of  $\gamma\delta$ T cells toward target MM cells treated with ZOL.

© 2015 Elsevier Inc. All rights reserved.

## 1. Introduction

$\gamma\delta$ T cell receptor (TCR)-positive T cells, which control the innate immune system, display anti-tumor immunity as well as other non-

**Abbreviations:** TCR, T cell receptor; N-BP, nitrogen-containing bisphosphonate; MM, multiple myeloma; IPP, isopentenyl pyrophosphate; ZOL, zoledronic acid; MIC-A, MHC class I-related chain gene A;  $\mu$ TAS, micro total analysis system; r, recombinant; h, human; IL, interleukin; HPLC, high-performance liquid chromatography; PB, peripheral blood; PBMC, peripheral blood mononuclear cell; CM, conditioned medium; ECI, Effective Chemotaxis Index; HPLC-MS/MS, high-performance liquid chromatography–tandem mass spectrometry; MRM, multiple reaction monitoring; DMAPP, dimethylallyl pyrophosphate; E:T ratio, effector cell to tumor cell ratio.

\* Corresponding author. 5 Nakachi, Yamashina-ku, Kyoto, 607-8414, Japan.

E-mail address: [ash@mb.kyoto-phu.ac.jp](mailto:ash@mb.kyoto-phu.ac.jp) (E. Ashihara).

<sup>1</sup> These authors contributed equally.

<http://dx.doi.org/10.1016/j.bbrc.2015.05.118>

0006-291X/© 2015 Elsevier Inc. All rights reserved.

immune-mediated anti-cancer effects. We have previously demonstrated that nitrogen-containing bisphosphonate (N-BP) treatment expands  $\gamma\delta$ T cells *ex vivo* and that these expanded cells can kill tumor cells in a major histocompatibility complex (MHC)-unrestricted manner [1–3]. N-BP inhibits farnesyl pyrophosphate synthase in the mevalonate pathway, resulting in the accumulation of isopentenyl pyrophosphate (IPP) [4], which is a stimulatory antigen for  $\gamma\delta$ T cells.  $\gamma\delta$ T cells stimulated by the N-BP zoledronic acid (ZOL) recognize tumor cells via several molecules including IPP, MHC class I-related chain gene A (MICA), ICAM-1, CD166, and CD266 [2,5–8].

Following the Encyclopedia of DNA Elements Projects, the analyses of proteomes as well as cellomes have attracted considerable attention across the life science. Research in these fields has recently focused on the elucidating vital mechanisms for the

development of novel therapeutic strategies against various diseases. Essential in parallel is the development of new devices for clarifying the mechanisms of cellular functions, including chemotaxis and secretion of hormones. A transwell chamber system has traditionally been used to analyze cell migration toward stimulators. However, this device is often inadequate in providing a reproducible, controllable, and stable linear gradient. Furthermore, a transwell chamber system is not compatible with live cell imaging [9,10]. To overcome these problems, the lab-on-chip or micro total analysis system ( $\mu$ TAS) has been recently applied. A  $\mu$ TAS controls the microenvironment of cells, enabling their biological behaviors, including chemotaxis, differentiation, and cell–cell interactions, to be analyzed [10–13]. The microvalve is a particularly useful tool for investigating the fast-response of cells [10]. We have developed a micro total analysis system ( $\mu$ TAS)-based microfluidic cellular analysis device, which possesses a minute-volume (240 nL) chamber integrated with a microsample injector controlled by a microvalve that permits the injection of a small amount (several nL) of a solute [14,15]. We have previously demonstrated real-time monitoring of antibody secretion from B cells using this microchip [14]. Moreover, because of the minute size of this chamber, we can analyze the behavior of individual cells in response to stimulators, including drugs and chemokines. Importantly, fluid convection or stirring has no influence on a concentration gradient and the solute can consequently spread in a diffusion-dependent manner (Supplementary Fig. S1). In the present study, we investigated  $\gamma\delta$ T cell chemotaxis using a  $\mu$ TAS-based microchamber device. Our results show that ZOL-treated MM cells secrete the metabolite of mevalonate pathway IPP and that IPP activates the  $\gamma\delta$ T cell migration.

## 2. Materials and methods

### 2.1. Reagents

The human RPMI8226 MM cell line was purchased from the Deutsche Sammlung von Mikroorganismen und Zellkulturen GmbH (Braunschweig, Germany) and was cultured in RPMI1640 (Gibco, Tokyo, Japan) containing 10% heat-inactivated FCS (Gibco), L-glutamine (Gibco), and 1% penicillin-streptomycin (Gibco). The synthetic pyrophosphomonoester compound 2-methyl-3-butenyl-1-pyrophosphate was kindly provided by Dr. Yoshimasa Tanaka (Kyoto University, Kyoto, Japan). Recombinant human interleukin-2 (rhIL-2) was provided by Shionogi Inc. (Tokyo, Japan). IPP, ammonium bicarbonate ( $\text{NH}_4\text{HCO}_3$ ), and 28% ammonia solution were purchased from Sigma–Aldrich (St. Louis, MO, USA). High-performance liquid chromatography (HPLC) grade 2-propanol and acetonitrile were obtained from Wako Pure Chemical Industries Ltd. (Osaka, Japan). All other chemicals used were of analytical-reagent grade.

### 2.2. Human $\gamma\delta$ T cell preparations and culture

Peripheral blood (PB) and human AB serum were collected from healthy volunteers. Approval was obtained from the institutional review board at Kyoto University Hospital and informed consent was provided by all volunteers, according to the Declaration of Helsinki. PB mononuclear cells (PBMCs) were isolated using Ficoll–Paque Plus (GE Healthcare, Tokyo, Japan). The PBMCs were then cultured and  $\gamma\delta$ T cells were expanded using 2-methyl-3-butenyl-1-pyrophosphate and rhIL-2, as described previously [2]. This method ensured expanded PBMC preparations that consisted predominantly of  $\gamma\delta$ T cells (>95%). These cells served as a polyclonal  $\gamma\delta$ T-cell source [2,8].

### 2.3. Preparation of N-BP stimulated RPMI8226 cell-conditioned medium

To investigate whether the supernatant of RPMI8226 MM cells treated with ZOL induced chemotaxis of  $\gamma\delta$ T cells using a  $\mu$ TAS-based microchamber [14,15], RPMI8226 MM cells were cultured with ZOL (1  $\mu\text{M}$ ) overnight. The conditioned medium (CM) was then collected and passed through a 0.22  $\mu\text{m}$  filter (Millipore, Tokyo, Japan). Human  $\gamma\delta$ T cells were obtained by culturing PBMCs, as previously reported [2]. These cells were cultured in the microchip and 24 nL of the CM supernatant was injected via a microinjector. After injection of the CM,  $\gamma\delta$ T cell migration was observed under a microscope and continuous time-lapse recording was performed in every 30 s for 30 min.

### 2.4. Quantitative analysis of $\gamma\delta$ T cell migration in a modified Boyden chamber assay

Prior to applying the  $\mu$ TAS-based microchamber system, the migration of  $\gamma\delta$ T cells was first confirmed in a modified Boyden chamber migration assay using 3.0  $\mu\text{m}$  porous membrane transwell inserts (Corning, Tokyo, Japan).  $\gamma\delta$ T cells ( $5 \times 10^4/\text{mL}$ ) were put into upper transwell chambers and IPP was added to the lower chambers at a final concentration of 1 or 5 ng/mL. After 4 h incubation,  $\gamma\delta$ T cells migrated into the lower chambers were counted by the modified MTT assay-based Cell-Counting Kit-8 (Dojindo Laboratory, Kumamoto, Japan) in accordance with manufacturer's instructions.

### 2.5. Quantitative analysis of $\gamma\delta$ T cell migration using a microchamber assay

The migration of  $\gamma\delta$ T cells in the microchamber was examined under a microscope with continuous time-lapse recording as described above. The tracks of cell migration were traced using Image J, an image-processing program in the public domain. To estimate the migration of  $\gamma\delta$ T cells quantitatively, the following indices of chemotaxis were used (Supplementary Fig. S2): (1) Speed:  $d/\Delta t$ , (2) Effective Chemotaxis Index (ECI):  $d \times \cos\theta/\Delta t = \Delta x/\Delta t$ . The chemotactic indices of  $\gamma\delta$ T cells were evaluated according to these formulae.

### 2.6. Measurement of IPP in culture supernatants

The concentrations of IPP in culture supernatants were determined using a sensitive HPLC-tandem mass spectrometry (HPLC-MS/MS) methods [16], as described previously, with slight modification. In brief, culture supernatants were added to 1 mL of 2-propanol:0.1 M  $\text{NH}_4\text{HCO}_3$  (1:1 v/v) and 1.5 mL of acetonitrile for deproteinization, and then vortexed. The deproteinized samples were kept for 10 min on ice, and then centrifuged for 20 min at 3000 rpm under 4 °C. After centrifugation, supernatants were transferred to glass tubes and then dried under a stream of nitrogen at room temperature. The residues were then dissolved in 40  $\mu\text{L}$  of 0.01 M  $\text{NH}_4\text{OH}$ , and 20  $\mu\text{L}$  aliquot of the solution was injected into the HPLC-MS/MS system. Quantification of IPP was performed by standard addition method. The HPLC system consisted of a gradient pump, a vacuum degasser, a column temperature controller, and an autosampler (Shimadzu, Kyoto, Japan). Column temperature was thermostat-controlled at 30 °C. The samples were injected onto a  $2.0 \times 50$  mm Luna C18(2) column, 3  $\mu\text{m}$  in particle diameter (Phenomenex, Torrance, CA). The IPP were chromatographed by a linear gradient between solution A (20 mM  $\text{NH}_4\text{HCO}_3$  and 0.1% triethylamine) and solution B (acetonitrile and 0.1% triethylamine). The gradient was as follows: 0–5 min, 100% A to 20% A; 5–7 min,

20% A; 7–7.01 min, 20% A to 100% A; 7.01–10 min, 100% A; equilibration with 100% A. The flow rate was set at 0.4 mL/min. Mass spectrometry (MS) detection was performed with an API 3200 MS/MS system (Applied Biosystems, Foster City, CA) in the negative electrospray ionization mode. The ion spray voltage was set at 4500 V, the capillary temperature was 700 °C and the collision energy was –42 eV. IPP was detected with the mass spectrometer in the multiple reaction monitoring (MRM) mode set at  $m/z$  244.80 →  $m/z$  79.00. The HPLC-MS/MS method could not separate and identify the isoforms of IPP and dimethylallyl pyrophosphate (DMAPP) in a similar manner as reported previously [16]. Therefore, the concentration was expressed as the total amount of IPP in the total amount of IPP and DMAPP (IPP/DMAPP).

## 2.7. Statistics

The differences in the speed of  $\gamma\delta$ T cell migration were analyzed using the *t* test. The dose-dependent effect of IPP on  $\gamma\delta$ T cell migration in conventional transwell chambers was analyzed using Williams' method. A *P*-value of 0.05 was considered statistically significant.

## 3. Results

### 3.1. Migration of $\gamma\delta$ T cells was activated by RPMI8226 CM

To investigate whether RPMI8226 MM cells treated with ZOL secreted chemotactic factors for  $\gamma\delta$ T cells, the CM from RPMI8226 cells treated by ZOL was applied into a microchamber containing  $\gamma\delta$ T cells ( $5 \times 10^5$ /mL) via a microinjector. After the injection of the CM, the  $\gamma\delta$ T cell migration was investigated under a microscope and the continuous time-lapse recording was carried out. While  $\gamma\delta$ T cells treated by the 10% FCS-containing culture medium (control) moved randomly (Supplementary Movie S1), the cells treated by the RPMI8226 CM migrated toward the injector (Fig. 1a and Supplementary Movie S2). Moreover, the number of cells with an ECI of  $>1 \mu\text{m}/\text{min}$  was increased by the injection of CM, compared to the control (Fig. 1b). The speed and ECI of RPMI8226 CM-treated  $\gamma\delta$ T cells ( $n = 84$ ) were  $2.69 \pm 0.81 \mu\text{m}/\text{min}$  and  $0.89 \pm 0.66 \mu\text{m}/\text{min}$ , respectively vs.  $2.0 \pm 0.69 \mu\text{m}/\text{min}$  and  $0.22 \pm 0.53 \mu\text{m}/\text{min}$ , respectively in the control of  $\gamma\delta$ T cells ( $n = 39$ ). The speed and ECI of  $\gamma\delta$ T cells after the injection of CM were significantly higher than

after the injection of the culture medium ( $P < 0.0001$ , Fig. 1c). In addition, after treatment with RPMI8226 CM, the  $\gamma\delta$ T cells moved closer to the injector than they did when treated with the control medium (Supplementary Fig. S3). These observations suggest that CM from ZOL-treated RPMI8226 cells contains certain chemotactic factors for  $\gamma\delta$ T cells.

Supplementary video related to this article can be found at <http://dx.doi.org/10.1016/j.bbrc.2015.05.118>.

### 3.2. IPP significantly increased the speed of $\gamma\delta$ T cell migration

We next investigated whether IPP, a metabolite of the mevalonate pathway and known  $\gamma\delta$ T cell stimulatory antigen, activates the  $\gamma\delta$ T cell migration. First we examined the effect of IPP on  $\gamma\delta$ T cell migration using a conventional transwell migration assay in a modified Boyden chamber. By counting the number of  $\gamma\delta$ T cells attracted across the transwell membrane to the lower chamber containing IPP (0, 1 or 5 ng/mL), we determined that IPP induced  $\gamma\delta$ T cell migration in a dose-dependent manner ( $P < 0.05$ , Supplementary Fig. S4). Next, we investigated the alteration in speed of the  $\gamma\delta$ T cells in response to IPP using the  $\mu$ TAS-based microchamber. We recorded the movement of  $\gamma\delta$ T cell migration and traced their tracks by IPP and the solvent control, and then estimated the chemotactic indices of  $\gamma\delta$ T cells. When the solvent control was injected,  $\gamma\delta$ T cells moved at random. In contrast, the  $\gamma\delta$ T cells moved toward the microinjector when IPP was introduced (Fig. 2a and Supplementary Movies S3 and Supplementary Movies S4). Like the treatment of RPMI8226-CM supernatant, the numbers of cells whose ECIs were more than  $1 \mu\text{m}/\text{min}$  were increased by the injection of IPP compared with that by the injection of the solvent control (Fig. 2b). The speed and ECI of IPP-treated  $\gamma\delta$ T cells ( $n = 51$ ) were  $2.89 \pm 0.80$  and  $1.29 \pm 0.80 \mu\text{m}/\text{min}$ , respectively. On the contrary, the speed and ECI of solvent-treated  $\gamma\delta$ T cells ( $n = 53$ ) were  $1.92 \pm 0.89$  and  $0.19 \pm 0.43 \mu\text{m}/\text{min}$ , respectively. IPP significantly enhanced the  $\gamma\delta$ T cell migration ( $P < 1 \times 10^{-5}$ ; Fig. 2c). After the injection of IPP, the  $\gamma\delta$ T cells moved further toward injector than the cells treated with solvent control (Supplementary Fig. S5). These findings indicate that IPP significantly enhances the chemotactic migration of  $\gamma\delta$ T cells.

Supplementary video related to this article can be found at <http://dx.doi.org/10.1016/j.bbrc.2015.05.118>.

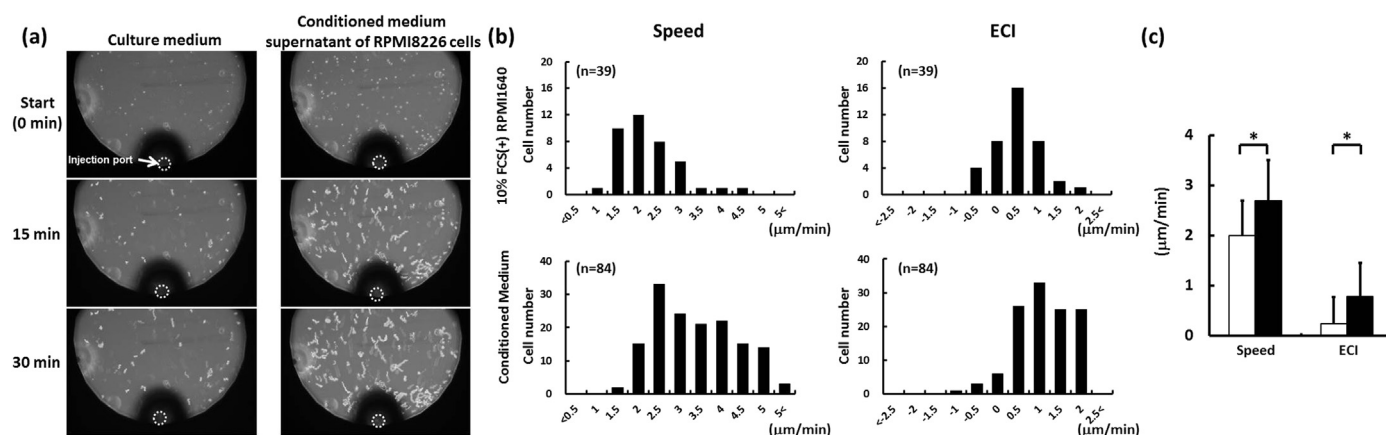


**Fig. 1.** Quantitative analysis of  $\gamma\delta$ T cell migration induced by RPMI8226-conditioned medium (CM). (a) Tracking  $\gamma\delta$ T cell migration after injection of the 10% FCS-containing culture medium or RPMI8226-CM via the microinjector. Images were captured every 30 s for the indicated times and overlaid. White tracks indicate each  $\gamma\delta$ T cell movement in the time during the indicated time. (b) Histograms of speed and effective chemotaxis index (ECI) of migrating  $\gamma\delta$ T cells. The negative values for speed and ECI indicate  $\gamma\delta$ T cell migration from the initial point in the opposite direction of the microinjector. (c) The mean values of speed and ECI of the  $\gamma\delta$ T cells treated with the medium (white bars) and with RPMI8226-CM (black bars) from the data in b. The data represent means + standard deviations and are representative data of four independent experiments. \* $P < 0.0001$ .

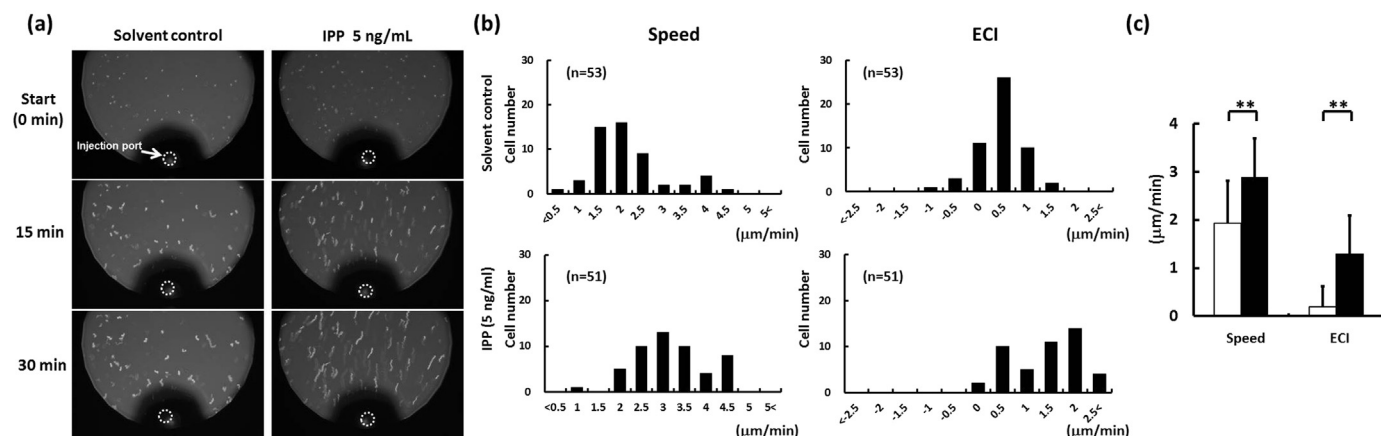


**Fig. 2.** Quantitative analysis of  $\gamma\delta$ T cell migration induced by Isopentenyl pyrophosphate (IPP). (a) Tracking  $\gamma\delta$ T cell migration after treatment with 5 ng/mL IPP-containing control solvent or control solvents. White tracks indicate each  $\gamma\delta$ T cell movement. (b) Histograms of speed and effective chemotaxis index (ECI) of migrating  $\gamma\delta$ T cells. The negative values for speed and ECI indicate  $\gamma\delta$ T cell migration from the initial points in the opposite direction of the microinjector. (c) The mean values of speed and ECI of migrating  $\gamma\delta$ T-cells induced by IPP (black bars) or solvent control (white bars) from the data in b. The data represent means + standard deviations and are representative data of two independent experiments.  $^{**}P < 1 \times 10^{-5}$ .

### 3.3. ZOL-treated RPMI8226 MM cells secreted IPP into the culture medium

Treatment of tumor cells with N-BPs inhibits farnesyl pyrophosphate synthase in the mevalonate pathway, resulting in the accumulation of the  $\gamma\delta$ T-cell stimulatory antigen IPP [4,17]. To determine whether the RPMI8226 MM cells secrete IPP into the supernatant by the ZOL treatment, we measured the IPP concentrations in the supernatants using HPLC-MS/MS as previously described [16]. Although IPP was not detected in the fresh medium containing 10% FCS, the concentrations of IPP in the culture supernatant without ZOL treatment were  $1.06 \pm 0.02$  ng/mL. When the cells were cultured in the presence of ZOL at 1  $\mu$ M and 5  $\mu$ M, the concentrations of IPP in the supernatant were  $3.24 \pm 0.27$  ng/mL and  $6.15 \pm 0.84$  ng/mL, respectively (Fig. 3). The IPP concentrations were increased by ZOL treatment in a dose-dependent manner. We also detected IPP in the supernatant of SBC-5 small lung cancer cells. The concentrations of IPP in the supernatant in the presence of ZOL at 0, 1, and 5  $\mu$ M were  $0.60 \pm 0.45$ ,  $0.79 \pm 0.43$ , and  $1.05 \pm 0.39$  ng/mL, respectively. Taken together, RPMI8226 MM

cells secrete IPP into the extracellular fluid by ZOL treatment, and  $\gamma\delta$ T cells migrate toward RPMI8226 cells by the secreted IPP.

## 4. Discussion

By N-BP treatment, IPP was accumulated on the surface of the tumor cells and IPP activates  $\gamma\delta$ T cells via  $\gamma\delta$ TCRs [1,2,3,4,8,18,19]. In a previous study, we have observed that migrating  $\gamma\delta$ T cells increase their speed toward MM as well as solid cancer target cells as they move closer to them [1,2], and from this we hypothesized that cancer cells secreted the chemotactic factors for  $\gamma\delta$ T cells into the supernatant. We focused on the ZOL-stimulated metabolites in the  $\gamma\delta$ T cells, and we detected IPP in the culture medium of RPMI8226 MM cells by ZOL treatment in a dose-dependent manner (Fig. 3). The previous study demonstrated that high doses of ZOL (more than 10  $\mu$ M) inhibited the prenylation of Rap1A in tumor cells [20]. Although the unprenylated Rap1A could be detected scarcely by the ZOL treatment at the concentration of 1  $\mu$ M, the treatment of ZOL at 1 and 5  $\mu$ M inhibited the prenylation (Supplementary Fig. S6). Therefore, farnesyl pyrophosphate synthase was inhibited by the treatment of ZOL at low doses of 1 and 5  $\mu$ M, resulting in the IPP secretion from RPMI8226 MM cells as shown in Fig. 3.

In the present study, using a  $\mu$ TAS-based microchamber, we have shown that CM from N-BP-treated RPMI8226 MM cells attracts  $\gamma\delta$ T cells toward the injection port, providing further evidence that suggests that RPMI8226 MM cells secrete  $\gamma\delta$ T cell chemotactic factors. It has been shown that the metabolite IPP accumulates in tumor cells following N-BP treatment, that it is recognized by  $\gamma\delta$ T cells and that it is a potential chemoattractive factor [4], therefore we focused our investigation of chemotactic factors secreted from MM cells on IPP. The conventional migration assay, using a modified Boyden chamber, showed that IPP induced  $\gamma\delta$ T cell migration in a dose-dependent manner. However, the possibility that  $\gamma\delta$ T cells activated by IPP move randomly and migrate toward the lower chamber of the Boyden system is not excluded, whereas our  $\mu$ TAS-based microchamber clearly demonstrated the chemotaxis of  $\gamma\delta$ T cells. Moreover, this microchamber enabled to observe that IPP also increased the speed of  $\gamma\delta$ T cell migration significantly.

The fact that this  $\mu$ TAS-based microchamber has a very small volume (240 nL) and that the concentration gradient in the chamber is not influenced by fluid convection or stirring gives the

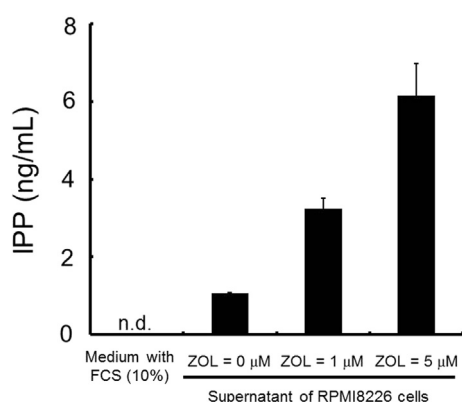


**Fig. 3.** Concentration of isopentenyl pyrophosphate (IPP) in the supernatant of RPMI8226 myeloma cells. Zoledronic acid was added to  $1 \times 10^6$  cells at the indicated concentration and the cells were cultured for 18 h. The concentration of IPP in the supernatant was then determined by high-performance liquid chromatography-tandem mass spectrometry. The data represent means + standard deviation of two independent experiments. n.d.; not detected.



system two unique characteristics. Firstly, cell migration can be analyzed in a short period because of the minute chamber and microinjector [10]. Recently, Benzaïd et al. demonstrated that IPP induced  $\gamma\delta$ T cell migration using a conventional transwell migration assay [17]. We confirmed the IPP-induced migration of  $\gamma\delta$ T cells also in this study. The incubation times prior to evaluation of migration by Benzaïd and colleagues and in our transwell experiments are 24 and 4 h, respectively. However, using a microchamber, we could detect the migration of  $\gamma\delta$ T cells only within 30 min. Moreover, this microchamber analysis revealed that IPP dramatically enhanced  $\gamma\delta$ T cell migration compared with the analysis used the transwell chamber. The minute size of our chamber means that the profile of the concentration gradient within it remains more stable than in the conventional transwell chamber [10]. Moreover, our  $\mu$ TAS-based microchamber enables us to observe live cell image under a microscope [10]. Consequently, we were able to detect migration directly for 30 min and analyze their chemotaxis statistically in <100 cells. The second unique characteristic of this  $\mu$ TAS-based microchamber is its ability to mimic secretion of a humoral factor from the cell surface. A solute injected via a microinjector can spread in a diffusion-dependent manner; thus, microinjection of a humoral factor mimics its release from a cell's surface (Fig. 4). This microchamber is therefore able to mimic the microenvironment in the immediate vicinity of the introduced cells.

In conclusion, we have demonstrated the activation of  $\gamma\delta$ T cell migration using a  $\mu$ TAS-based microchamber. IPP, the mevalonate metabolite increased by ZOL treatment, activates  $\gamma\delta$ T cell migration. There have been many clinical studies and clinical trials of immunotherapy against cancers using  $\gamma\delta$ T-cells, but the outcomes have not necessarily been satisfactory [21–23]. It is expected that the higher the effector cell to tumor cell (E:T) ratio, the greater the cytotoxic impact on the tumor; however, increasing the E:T ratio in the clinical setting has limits because of adverse effects. Our observations suggest that cancer cells treated ZOL secrete IPP, which leads to their death via  $\gamma\delta$ T cell killing. In other words, the metabolite IPP induced by ZOL is a suicide factor. This limitation may be overcome if  $\gamma\delta$ T-cells can be stimulated to reach target tumor tissues more locally.

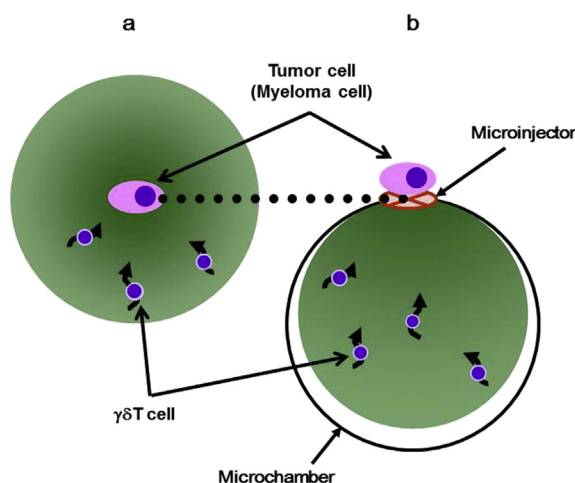


**Fig. 4.** Scheme of the  $\mu$ TAS-based microchamber mimicking the secretion of humoral factor released from the myeloma cell surface. (a) The secreted humoral factor spreads from the cell surface into the microenvironment in a diffusion-dependent manner. (b) The solute introduced via a microinjector can spread within the microchamber in a diffusion-dependent manner, mimicking the spread of humoral factor secreted from the myeloma cell surface. The gradient of color (gray) indicates that of the secreted humoral factor.  $\gamma\delta$ T cells migrate in accordance with the gradient of the secreted humoral factor.

## Conflict of interest statements

Conflict-of-interest disclosure: E. Ashihara, S. Kimura, Y. Nakagawa, H. Hirai, T. Miida, S. Yamato, S. Shoji, and Taira Maekawa disclose no financial conflict of interest. T. Munaka, M. Kanai, and H. Abe. are employees of Shimadzu Corporation.

## Acknowledgments

This work was supported by a Grant-in-Aid from the Ministry of Education, Culture, Sports, Science and Technology (MEXT) in Japan (23591404, 26461436 to EA, 21591201 to SK, 24790175 to SN, 25461615, 11068019 to HH, and 23112507, 24390244, 25112706, 11068019 to TM). This work was also supported by Mitsubishi Pharma Medical Research Foundation (The 26th Grants for Basic Research of Hematology to EA), the Kobayashi Foundation for Cancer Research (The 6th Grants for Clinical Research of Oncology to TM), a Grant from Takeda Science Foundation (The Grants 2011 for Basic Research of Medical Science to HH), and the Research Grant of the Princess Takamatsu Cancer Research Fund (13-24521 to TM).

## Appendix A. Supplementary data

Supplementary data related to this article can be found at <http://dx.doi.org/10.1016/j.bbrc.2015.05.118>.

## Transparency document

Transparency document related to this article can be found online at <http://dx.doi.org/10.1016/j.bbrc.2015.05.118>.

## References

- [1] K. Sato, S. Kimura, H. Segawa, A. Yokota, S. Matsumoto, J. Kuroda, M. Nogawa, T. Yuasa, Y. Kiyono, H. Wada, T. Maekawa, Cytotoxic effects of gammadelta T cells expanded ex vivo by a third generation bisphosphonate for cancer immunotherapy, *Int. J. Cancer* 116 (2005) 94–99.
- [2] R. Uchida, E. Ashihara, K. Sato, S. Kimura, J. Kuroda, M. Takeuchi, E. Kawata, K. Taniguchi, M. Okamoto, K. Shimura, Y. Kiyono, C. Shimazaki, M. Taniwaki, T. Maekawa, Gamma delta T cells kill myeloma cells by sensing mevalonate metabolites and ICAM-1 molecules on cell surface, *Biochem. Biophys. Res. Commun.* 354 (2007) 613–618.
- [3] T. Yuasa, K. Sato, E. Ashihara, M. Takeuchi, S. Maita, N. Tsuchiya, T. Habuchi, T. Maekawa, S. Kimura, Intravesical administration of gammadelta T cells successfully prevents the growth of bladder cancer in the murine model, *Cancer Immunol. Immunother.* 58 (2009) 493–502.
- [4] H.J. Gober, M. Kistowska, L. Angman, P. Jenö, L. Mori, G. De Libero, Human T cell receptor gammadelta cells recognize endogenous mevalonate metabolites in tumor cells, *J. Exp. Med.* 197 (2003) 163–168.
- [5] H. Das, V. Groh, C. Kuijl, M. Sugita, C.T. Morita, T. Spies, J.F. Bukowski, MICA engagement by human Vgamma2Vdelta2 T cells enhances their antigen-dependent effector function, *Immunity* 15 (2001) 83–93.
- [6] Y. Kato, Y. Tanaka, M. Hayashi, K. Okawa, N. Minato, Involvement of CD166 in the activation of human gamma delta T cells by tumor cells sensitized with nonpeptide antigens, *J. Immunol.* 177 (2006) 877–884.
- [7] O. Toutirais, F. Cabillat, G. Le Friec, S. Salot, P. Loyer, M. Le Gallo, M. Desille, C.T. de La Pintiére, P. Daniel, F. Bouet, V. Catros, DNAX accessory molecule-1 (CD226) promotes human hepatocellular carcinoma cell lysis by Vgamma9Vdelta2 T cells, *Eur. J. Immunol.* 39 (2009) 1361–1368.
- [8] S. Yamashita, Y. Tanaka, M. Harazaki, B. Mikami, N. Minato, Recognition mechanism of non-peptide antigens by human gammadelta T cells, *Int. Immunol.* 15 (2003) 1301–1307.
- [9] B.J. Kim, M. Wu, Microfluidics for mammalian cell chemotaxis, *Ann. Biomed. Eng.* 40 (2012) 1316–1327.
- [10] T.M. Keenan, A. Folch, Biomolecular gradients in cell culture systems, *Lab. Chip* 8 (2008) 34–57.
- [11] M.L. Kovarik, P.C. Gach, D.M. Orloff, Y. Wang, J. Balowski, L. Farrag, N.L. Allbritton, Micro total analysis systems for cell biology and biochemical assays, *Anal. Chem.* 84 (2012) 516–540.
- [12] C.T. Culbertson, T.G. Mickleburgh, S.A. Stewart-James, K.A. Sellens, M. Pressnall, Micro total analysis systems: fundamental advances and biological applications, *Anal. Chem.* 86 (2014) 95–118.
- [13] E.K. Sackmann, A.L. Fulton, D.J. Beebe, The present and future role of microfluidics in biomedical research, *Nature* 507 (2014) 181–189.

- [14] T. Munaka, H. Abe, M. Kanai, T. Sakamoto, H. Nakanishi, S. Shoji, S. Kimura, T. Maekawa, A. Murakami, Real-time monitoring of antibody secretion from B-cells on a microchip stimulated with a minute amount of mitogen, *Analyst* 132 (2007) 512–514.
- [15] M. Kanai, H. Abe, T. Munaka, Y. Fujiyama, D. Uchida, A. Yamayoshi, H. Nakanishi, A. Murakami, S. Shoji, Micro chamber for cellular analysis integrated with negligible dead volume sample injector, *Sensors Actuators A: Phys.* 114 (2004) 129–134.
- [16] L. Henneman, A.G. van Cruchten, S.W. Denis, M.W. Amolins, A.T. Placzek, R.A. Gibbs, W. Kulik, H.R. Waterham, Detection of nonsterol isoprenoids by HPLC-MS/MS, *Anal. Biochem.* 383 (2008) 18–24.
- [17] I. Benzaid, H. Monkkonen, V. Stresing, E. Bonnelye, J. Green, J. Monkkonen, J.L. Touraine, P. Clezardin, High phosphoantigen levels in bisphosphonate-treated human breast tumors promote Vgamma9Vdelta2 T-cell chemotaxis and cytotoxicity in vivo, *Cancer. Res.* 71 (2011) 4562–4572.
- [18] V. Lafont, J. Liautard, M. Sable-Teychene, Y. Sainte-Marie, J. Favero, Isopentenyl pyrophosphate, a mycobacterial non-peptidic antigen, triggers delayed and highly sustained signaling in human gamma delta T lymphocytes without inducing down-modulation of T cell antigen receptor, *J. Biol. Chem.* 276 (2001) 15961–15967.
- [19] B. Rincon-Orozco, V. Kunzmann, P. Wrobel, D. Kabelitz, A. Steinle, T. Herrmann, Activation of V gamma 9V delta 2 T cells by NKG2D, *J. Immunol.* 175 (2005) 2144–2151.
- [20] A.S. Idrees, T. Sugie, C. Inoue, K. Murata-Hirai, H. Okamura, C.T. Morita, N. Minato, M. Toi, Y. Tanaka, Comparison of gammadelta T cell responses and farnesyl diphosphate synthase inhibition in tumor cells pretreated with zoledronic acid, *Cancer Sci.* 104 (2013) 536–542.
- [21] Y. Abe, M. Muto, M. Nieda, Y. Nakagawa, A. Nicol, T. Kaneko, S. Goto, K. Yokokawa, K. Suzuki, Clinical and immunological evaluation of zoledronate-activated Vgamma9gammadelta T-cell-based immunotherapy for patients with multiple myeloma, *Exp. Hematol.* 37 (2009) 956–968.
- [22] J. Nakajima, T. Murakawa, T. Fukami, S. Goto, T. Kaneko, Y. Yoshida, S. Takamoto, K. Kakimi, A phase I study of adoptive immunotherapy for recurrent non-small-cell lung cancer patients with autologous gammadelta T cells, *Eur. J. Cardiothorac. Surg.* 37 (2010) 1191–1197.
- [23] A.J. Nicol, H. Tokuyama, S.R. Mattarollo, T. Hagi, K. Suzuki, K. Yokokawa, M. Nieda, Clinical evaluation of autologous gamma delta T cell-based immunotherapy for metastatic solid tumours, *Br. J. Cancer* 105 (2011) 778–786.